Pharmacology Research & Perspectives

WILEY | BRITISH PHARMACOLOGICAL SOCIETY

ORIGINAL ARTICLE OPEN ACCESS

(+)-Trans-Cannabidiol Is an Agonist at Human CB_2 Receptors

Pedro Bans Burtchaell[1,2] | Marina Junqueira Santiago[2] | Chenxi Wang[1,2] | Mehdi Hagdoost[3] | Evie J. M. Clay[4,5] | Dani Mohnot[2] | Mark Connor[2]

[1]School of Pharmacy and Pharmaceutical Sciences, Trinity College Dublin, University of Dublin, Dublin, Ireland | [2]Macquarie Medical School, Macquarie University, North Ryde, New South Wales, Australia | [3]Nalu Bio, San Francisco, California, USA | [4]School of Natural Sciences, Macquarie University, Sydney, New South Wales, Australia | [5]School of Biological Sciences, University of Bristol, Bristol, UK

Correspondence: Mark Connor (mark.connor@mq.edu.au)

Received: 29 May 2026 | **Revised:** 17 August 2026 | **Accepted:** 8 September 2026

Keywords: agonism | cannabinoid | chirality | G protein coupled receptor

ABSTRACT

(−)-*trans*-Cannabidiol ((−)-CBD) is a principal phytocannabinoid from *Cannabis sativa*. (−)-CBD has complex pharmacology but is a relatively weak inhibitor of CB_1 and CB_2 receptor signaling. Cannabidiol has two chiral centres and thus four stereoisomers. (+)-*trans*-CBD ((+)-CBD) has a higher affinity than (−)-CBD at CB_1 and CB_2, but its pharmacodynamic effects at these receptors are incompletely described. We examined the activity of (+)-CBD at human CB_1 and CB_2 receptors using a fluorescence-based assay of membrane potential in AtT20 cells stably expressing CB_1 or CB_2 receptors. (+)-CBD produced a rapid, concentration-dependent hyperpolarization in CB_2-expressing cells (pEC_{50} 6.63 ± 0.08) with a maximal effect 90% of the response to CP55940. The CB_2 response was blocked by pertussis toxin pretreatment and competitively inhibited by the CB_2 antagonist AM630 (Schild slope 1.1 ± 0.1). (+)-CBD was a low-efficacy, low-potency CB_1 agonist and inhibited somatostatin-receptor effects at high concentrations (10–30 μM). (+)-CBD had no effect on the membrane potential of AtT20 wild-type cells. *In silico* modeling of ligand interactions with CB_2 indicated that (+)-CBD but not (−)-CBD formed an H-bond with Ser285, a residue crucial for agonist activation of CB_2. Our data suggests (+)-CBD acted as a CB_2 agonist via the orthosteric binding site on the receptor. Synthetic CBD, including (+)-CBD, has previously been administered in clinical trials, presumably without consideration of its potential CB_2 agonist activity. Given the relative safety of (−)-CBD in people, (+)-CBD may be a useful drug to explore CB_2-sensitive disease states.

1 | Introduction

Cannabidiol is one of the major biologically active constituents of *Cannabis*, and is a drug used in the treatment of some seizure disorders, multiple sclerosis and chronic pain [1]. The mechanisms of action of CBD in these conditions remain poorly defined, although among the dozens of potential targets for CBD identified in vitro, interactions with ion channels [2–4], and G protein-coupled receptors [5–7] provide potentially plausible sites of action. CBD also affects drug-metabolizing enzymes [8, 9], leading to pharmacokinetic drug–drug interactions which may contribute to its clinical effects. CBD is generally described as a negative allosteric modulator of CB_1 receptors [10, 11] while there are contrasting reports of its activity at CB_2 [11–14].

CBD has 2 chiral centres, and thus 4 potential stereoisomers [15]. (−)-*trans*-CBD (Figure 1) is to date the only isomer found in *Cannabis*, which is in contrast to other chiral cannabinoids,

Abbreviations: CBC, cannabichromene; (+)-CBD, (+)-*trans*-cannabidiol; (−)-CBD, (−)-*trans*-cannabidiol; CD, circular dichroism; GIRK, G protein-gated inwardly rectifying K channels; HBSS, modified Hank's buffered saline solution; MPA, membrane potential assay; PTX, pertussis toxin; SRIF-14, somatostatin-14; SSTR, somatostatin receptors; THC, Δ^9-tetrahydrocannabinol.

as all 4 isomers of Δ^9-tetrahydrocannabinol (THC) have been identified in some strains of *Cannabis* [16, 17], as have both (−) and (+)-cannabichromene (CBC) [16, 18]. (+)-*trans*-CBD (Figure 1) can be readily accessed through synthetic routes [15, 19, 20], and a small number of studies have reported biological activities of (+)-CBD distinct from those of (−)-CBD. These include antagonism of CB_1-mediated responses at sub-μM (+)-CBD concentrations in mouse neurons in vitro, activation of human $S1P_1$ and $S1P_3$ receptors in HEK293 cells [21] and a substantially higher affinity of (+)-CBD for CB_2 receptors than CB_1 receptors [19].

CBD is currently being trialed in people to treat many conditions [22], presumably in part because of its relatively good safety profile and the strong anecdotal evidence about the efficacy of *Cannabis* for an extraordinarily wide range of ailments. It is not always clear what molecular form of CBD is used in the trials—plant derived CBD is likely to be (−)-*trans*-CBD, but if synthetic CBD is being used, then there is a possibility that (+)-CBD is being administered to patients as either a pure substance or part of a racemic mixture. Use of pure (+)-CBD was reported in one trial [23]; however, in other trials using synthetic CBD, the drug's chirality is not reported. Given the importance of chirality in cannabinoid action [17, 24, 25], and the moderate affinity of (+)-CBD for CB_2 receptors [19], we explored the activity of (+)-*trans*-CBD at cannabinoid receptors in vitro, finding that it has robust agonist activity at CB_2 receptors.

2 | Methods

2.1 | Cell Culture

AtT20-FlpIn cells stably expressing 3× haemagglutinin-tagged human CB_1 or CB_2 (AtT20-CB_1; AtT20-CB_2) [26] or untransfected AtT20-FlpIn cells (AtT20-WT; first described in [27]) were cultured in DMEM medium containing 10% FBS and 100 units penicillin–streptomycin (P/S) in a humidified incubator at 37°C with 5% CO_2. Media for AtT20-CB_1 and AtT20-CB_2 cells also contained the selection antibiotic hygromycin (80 μg.mL^{-1}). Cells were fed every 3–4 days and passaged when they had reached approximately 80% confluence. Cells were routinely tested for mycoplasma using MycoAlert detection kit (Lonza) and were always negative.

For experiments, Leibovitz's L-15 medium supplemented with 1% FBS, 100 units P/S, and 15 mM glucose was used. Cells were cultured overnight in a humidified incubator at 37°C, ambient air (no added CO_2).

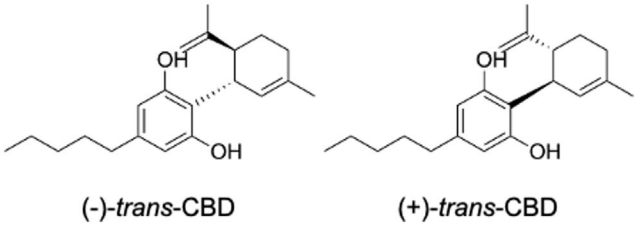

FIGURE 1 | Structures of (−)- and (+)-trans-CBD. The structures of (−) and (+)-CBD were imputed in Chemdraw from their SMILES keys.

2.2 | Membrane Potential Assay

Changes in membrane potential were measured using a proprietary membrane potential assay kit (MPA Blue #R8034, Molecular Devices, San Jose, CA, USA) as described previously [28]. AtT20-CB_1, AtT20-CB_2, or AtT20-WT cells were incubated overnight in 90 μL of L-15-supplemented medium in 96-well black-walled, clear-bottom plates (Corning). The same volume (90 μL) of MPA dye dissolved in a modified Hank's Buffered Saline Solution (HBSS) was added to the cells at 50% of the manufacturer's recommended concentration, then placed in a FlexStation 3 (Molecular Devices) for at least 60 min at 37°C. For single additions, drugs were dissolved in HBSS supplemented with 0.1% bovine serum albumin (Sigma-Aldrich) and were added in a volume of 20 μL (for a final volume of 200 μL) after a baseline recording of 60–120 s; for double additions the second addition was 22 μL. Fluorescence was recorded every 2 s with excitation at 530 nm and emission at 565 nm (550 nm cut-off).

Drug effects are reported as the peak change in fluorescence following drug addition, expressed as a percentage of the pre-drug baseline. Each column included one well in which only vehicle-control (buffer + DMSO) was added; the changes in fluorescence produced by these vehicle-control additions were subtracted from the experimental traces. The final DMSO concentrations in the well were between 0.1% (single addition) and 0.2% (double addition). Concentration-response parameters were derived from at least six independent experiments, performed in duplicate and then fitted to a 4-parameter logistic equation in GraphPad PRISM (version 10.3.1, RRID:SCR_002798). Values for *p*A2 and Schild slope were calculated for individual experiments in PRISM, and the values were averaged. Data is presented as mean ± SEM of at least six independent replicates; exact values are noted in the text. Statistical comparisons of untransformed values were made using an unpaired Student's *t*-test or an ordinary one-way ANOVA followed by Dunnett's multiple-comparisons test versus control (PRISM).

2.3 | In Silico Modeling

Structural templates of the CB_2 receptor were retrieved from the Protein Data Bank. A total of seven X-ray and cryo-EM structures (PDB IDs: 6PT0 [29], 8GUQ, 8GUR, 8GUT, 6KPF, 6KPC [30] and 5ZTY [31]) were evaluated. Among these, the 8GUR structure was selected as it provided the most accurate activity predictions for a benchmark set of active and decoy CB_2 ligands [32]. Protein preparation for molecular docking was performed using UCSF Chimera's (UCSF Chimera, RRID:SCR_004097) Dock Prep protocol. This included the removal of solvents, unbound ions, and the co-crystallized ligand. Incomplete side chains were reconstructed using the Dunbrack 2010 rotamer library [33], while missing hydrogen atoms were added and partial charges assigned using the AMBER ff99bsc0 force field [34]. Energy minimization of the receptor structure was omitted, as it did not enhance model performance on the active–decoy dataset. The binding site and docking grid were defined using AutoDockTools4 [35] with the following grid centre coordinates: $X = 135$, $Y = 145$, $Z = 168$. The 3D structures of (−)-CBD, (+)-CBD, and CP55940 were downloaded from PubChem [36] and geometry-optimized using the MMFF94s force field [37].

Molecular docking was performed using AutoDock Vina 1.2 [38]. During the docking method assessment, three scoring functions (Vina, Vinardo [39], and a recently reported custom empirical set [40]) were evaluated. The Vinardo scoring function, which demonstrated superior performance in distinguishing actives from decoys, was selected for subsequent docking analyses. A grid box size of $25 \times 25 \times 25$ Å^3 and an exhaustiveness value of 100 were applied to all docking calculations, as increasing exhaustiveness did not yield significant improvements in docking scores. For each ligand, the top three best-scoring poses were retained for further analysis and comparison.

2.4 | Drugs and HBSS Solution

(−)-*trans*-CBD was from the National Measurement Institute (North Ryde, Australia, reported purity 99.4% ± 0.6%), and is referred to as (−)-CBD throughout. The structures of (−) and (+)-CBD for Figure 1 were imputed in Chemdraw (version 26.0.0.6599, Revvity Signals Software) from their SMILES key. (+)-*trans*-CBD (2-[(1S,6S)-3-methyl-6-(1-methylethenyl)-2-cyclohexen-1-yl]-5-pentyl-1,3-benzenediol, referred to as (+)-CBD, reported purity 100%), AM630 (a CB2-prefering antagonist, 100 nM−10 μM) [26], rimonabant (SR141716A, a CB1-prefering antagonist) and CP55940 (a non-selective CB receptor agonist, 1 nM-10 μM) were from Cayman Chemical. ML297 (a GIRK channel activator, 30 μM) was from Sigma-Aldrich. Somatostatin-14 was from AUSPEP (Melbourne, Australia). Pertussis Toxin was from HelloBio (Bristol, UK).

In order to confirm that the (−)-CBD and (+)-CBD we used were indeed optical isomers, we obtained their respective spectra using circular dichroism (CD, Figure S1). Briefly, the circular dichroism and absorbance spectra of the samples were determined using the Jasco J-1500 spectropolarimeter (RRID:SCR_020147). Conditions were optimized prior to final readings. Samples of (+)-CBD and (−)-CBD were diluted to 0.1 mg.mL^{-1} in 100% ethanol and a pathlength of 0.1 mm was used. For each sample, 32 runs were carried out, and each curve represents the average of the 32 runs. The pure ethanol control reading was subtracted from the sample readings, and these blank-corrected readings were used to produce the spectra. Measurements were carried out at room temperature. Measurements were made twice with different samples of (−)-CBD and (+)-CBD, with similar results.

HBSS was prepared by mixing (mM) NaCl 145, HEPES 22, Na_2HPO_4 0.338, $NaHCO_3$ 4.17, KH_2PO_4 0.441, $MgSO_4$ 0.407, $MgCl_2$ 0.493, glucose 5.56, and $CaCl_2$ 1.26. The solution pH was adjusted to 7.4, and osmolarity was 315 ± 15 mOsmol.

3 | Results

3.1 | The Effects of (+)-CBD at AtT20-CB$_2$, CB$_1$ and WT

Application of (+)-CBD produced a rapid, concentration-dependent hyperpolarization of AtT20-CB$_2$ cells with a pEC$_{50}$ of 6.63 ± 0.08 (n_H 1.3 ± 0.3), and maximum change in fluorescence of 24.7% ± 0.9% (Figure 2A,B,E, blue closed-circle; $n = 7$). In comparison, the non-selective cannabinoid receptor agonist CP55940 hyperpolarised AtT20-CB2 cells with a pEC$_{50}$ of 7.48 ± 0.08 (n_H 1.2 ± 0.2) to a maximum of 27.2% ± 1.2% (Figure 2A,B,E, open-diamonds; $n = 6$). A brief application of (−)-CBD did not significantly affect the fluorescence of AtT20-CB2 cells (Figure 2B). The maximum change in fluorescence produced by 10 μM (−)-CBD was 4.3% ± 1.5%; this was not different to the change in fluorescence produced by vehicle in the same experiments (2.4% ± 0.5%, $p > 0.05$, unpaired Student's t-test, $n = 7$).

High concentrations of (+)-CBD produced a modest hyperpolarization of AtT20-CB$_1$ cells, with only 10 μM and 30 μM being significantly different from vehicle ($n = 7$, one-way ANOVA, $p > 0.001$, Figure 2C,E, blue open-circles). CP55940 hyperpolarised AtT20-CB$_1$ cells with a pEC$_{50}$ of 7.64 ± 0.08 (n_H 1.2 ± 0.3) to a maximum of 34.3% ± 1.6% (Figure 2C and Figure 2E, closed-diamonds). (+)-CBD (1–30 μM) did not produce a change in fluorescence in AtT20-WT cells that was different from vehicle-controls ($n = 11$, one-way ANOVA $p = 0.32$, Figure 2D,E, black squares).

The effects of (+)-CBD (10 μM) were significantly inhibited by pretreatment of AtT20-CB$_1$ or AtT20-CB$_2$ cells with pertussis toxin (200 ng.mL^{-1} overnight, $p < 0.05$ for each, $n = 7$; Figure 3).

3.2 | Quantification of CB$_2$ Receptor Antagonism

To further explore the interaction of (+)-CBD at CB$_2$ receptors, we conducted a Schild analysis using the CB$_2$ receptor antagonist AM630, and compared the effects of AM630 on (+)-CBD and its effects on the orthosteric agonist CP55940. Increasing concentrations of AM630 produced a similar parallel shift in the concentration response curves to both (+)-CBD (Schild slope 1.1 ± 0.1, (Figure 4A,B) and CP55940 (Schild slope 0.9 ± 0.1, Figure 4C,D), the pA$_2$ for AM630 was 6.5 ± 0.16 for (+)-CBD and 6.0 ± 0.17 for CP55940.

3.3 | CB$_1$ Receptor Antagonism

We examined whether a selective CB$_1$ antagonist, rimonabant, blocks (+)-CBD signal on human CB$_1$. A 5-min pretreatment of AtT20-CB$_1$ cells with rimonabant (3 μM) significantly reduced the signal of 10 μM (+)-CBD from 6.5% ± 1.1% to 1.1% ± 0.7% ($p < 0.05$, $n = 7$, Figure 5A). This pretreatment also blocked the effects of a submaximally effective concentration of CP55940 (100 nM), from 25.5% ± 1.4% to −2.0% ± 1.1% ($p < 0.05$, $n = 7$, Figure 4A).

(+)-CBD has previously been identified as a CB$_1$ antagonist in mouse neurons [21]. We determined that high concentrations of (+)-CBD (10 μM, 30 μM) produced a significant inhibition of responses to a high concentration of CP55940 (300 nM) ($n = 7$, one-way ANOVA $p > 0.001$, Figure 5C,D). However, pretreatment of AtT20-CB$_1$ cells with a concentration of (+)-CBD (1 μM) that produced no change in membrane potential by itself had no effect on the response to subsequently applied CP55940, as

shown in Figure 5B (CP55940 alone; pEC_{50} 7.75 ± 0.08, maximum response 29.9 ± 1.1, n_H 1.2 ± 0.2; CP55940 in the presence of 1 μM (+)-CBD; 7.68 ± 0.08, maximum response 29.6 ± 1.2, n_H 1.1 ± 0.2, $n = 6$).

3.4 | Other Effects of (+)-CBD

In AtT20-CB_1 cells, the apparent effects of (+)-CBD on responses to a high efficacy agonist could arise from actions at

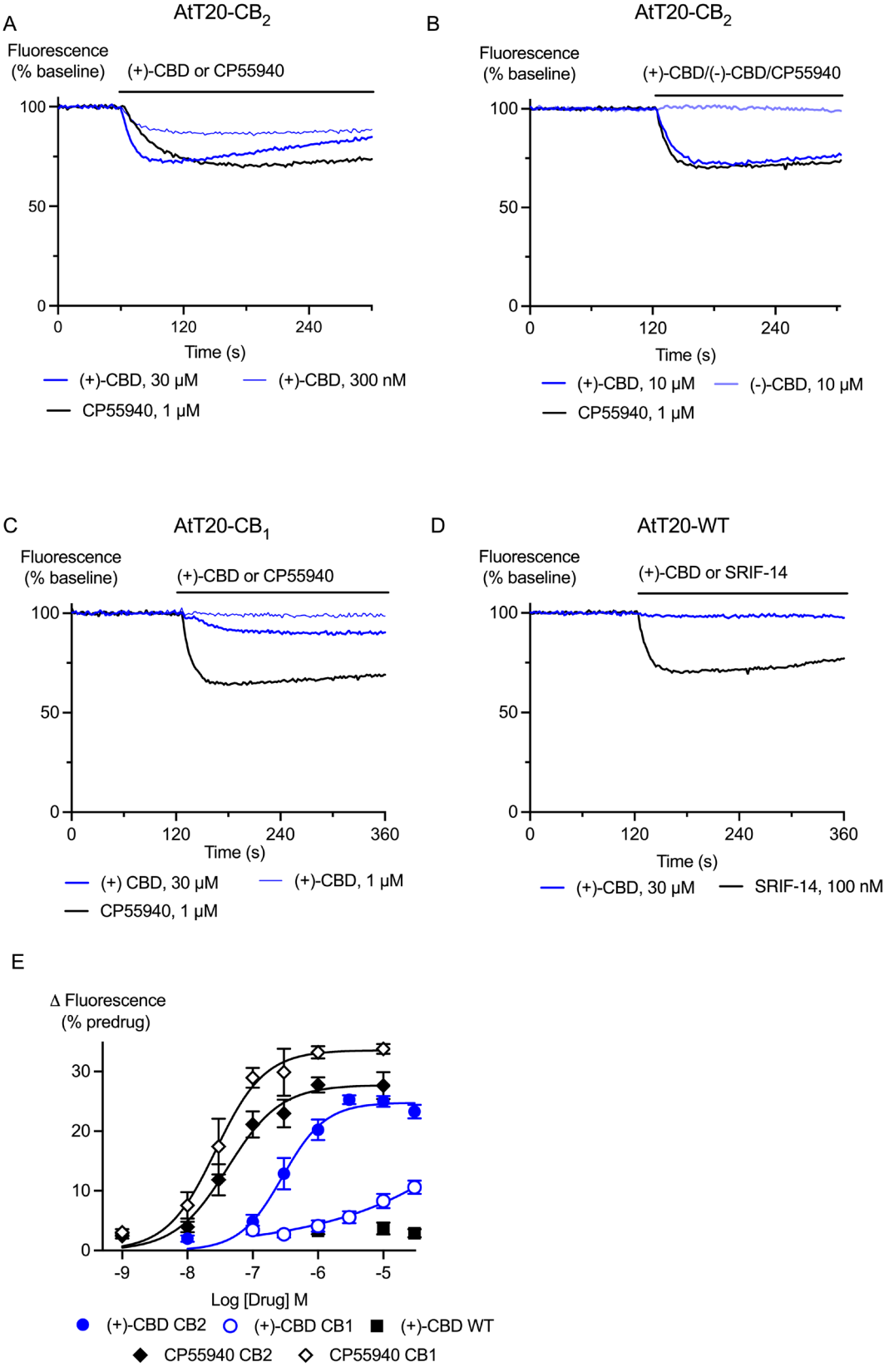

FIGURE 2 | Legend on next page.

FIGURE 2 | (+)-CBD hyperpolarises AtT20-CB_2 and AtT20-CB_1 cells. AtT20 cells expressing CB_2, CB_1 or no cannabinoid receptors (WT) were challenged with (+)-CBD and CP55940. A fluorescent membrane potential dye was used to measure the response. (A) Representative traces showing that application of (+)-CBD (300 nM, 30 μM) and CP55940 (1 μM) to AtT20-CB_2 cells produced a sustained decrease in fluorescence, consistent with hyperpolarization of the cells. (B) Representative traces showing that application of (+)-CBD (10 μM) and CP55940 (1 μM) but not (−)-CBD (10 μM) to AtT20-CB_2 cells produced a sustained decrease in fluorescence. (C) Representative traces showing that application of (−)-CBD (10 μM, 30 μM) to AtT20-CB_1 cells produced much smaller change in fluorescence than CP55940 (1 μM). (D) Representative traces showing that (+)-CBD (30 μM) did not produce a change in fluorescence in AtT20-WT cells, but somatostatin-14 (SRIF-14, 100 nM) did. (E) Concentration-response curves for (+)-CBD, and CP55940 showing the maximum change in fluorescence produced by each drug in AtT20-CB_1, -CB_2, and -WT cells. Each point represents the mean ± SEM of at least 6 independent experiments, performed in duplicate.

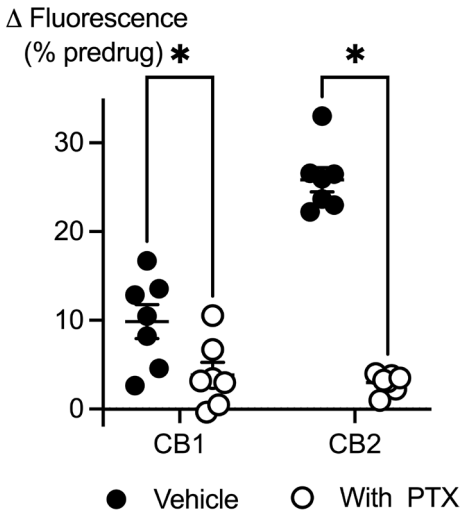

FIGURE 3 | Effects of (+)-CBD are mediated via pertussis toxin-sensitive G proteins. AtT20 cells expressing CB_1 or CB_2 receptors were challenged with (+)-CBD (30 μM) after overnight pretreatment with pertussis toxin (PTX, 200 ng.mL^{-1}) or vehicle. The effects of (+)-CBD were significantly (*) reduced by PTX (Student's unpaired *t*-test, $p < 0.05$). Each dot represents one independent experiment performed in duplicate; bars indicate mean ± SEM ($n = 7$).

the CB_1 receptor or actions at the signaling effector, G protein-gated inwardly rectifying K channels (GIRK channels). We tested the latter possibility in two ways: by pre-incubating AtT20-WT cells with (+)-CBD (1–30 μM) and then activating GIRK channels via endogenous somatostatin receptors (SSTR), and by directly activating GIRK channels with ML297 following pre-incubation with (+)-CBD. (+)-CBD (10 μM, 30 μM) inhibited the hyperpolarization produced by 100 nM somatostatin-14 (SRIF-14; $n = 6$, one-way ANOVA $p = 0.0027$, Figure 6A,B) and by 30 μM ML297 (one-way ANOVA $p = 0.025$, Figure 6C,D). At 30 μM, (+)-CBD inhibited the activation of GIRK by SRIF-14 by 41% ± 4% and the direct activation of GIRK by ML297 by 14% ± 2%, suggesting that (+)-CBD directly inhibits SSTR in addition to GIRK.

In contrast to (+)-CBD, 5 min application of (−)-CBD (10 μM, 30 μM) produced a small apparent hyperpolarization of AtT20-WT cells ($n = 11$, one-way ANOVA $p < 0.0001$, Figure 7A) but did not inhibit the hyperpolarization of AtT20-WT cells by 100 nM SRIF-14 ($n = 8$, one-way ANOVA $p = 0.8344$, Figure 7B,D). (−)-CBD (30 μM) also failed to inhibit the hyperpolarization produced by 30 μM ML297 ($n = 7$, one-way ANOVA $p = 0.3869$, Figure 7C,E).

3.5 | (+)-*CBD and* (−)-CBD *Docking in Human* CB_2 *Receptor*

Molecular docking simulations were conducted to investigate the differences in how the enantiomers of CBD interact with the CB_2 receptor (Figure 8). The results revealed a notable difference in docking scores: (+)-CBD exhibited a more favorable binding affinity (−8.224 kcal/mol) compared to (−)-CBD (−7.414 kcal/mol). A key distinction in their binding modes was observed in the interaction with the amino acid residue Ser285. In the top-ranked binding pose, one of the hydroxyl groups of (+)-CBD formed a moderately strong hydrogen bond with Ser285, with an oxygen–oxygen (O–O) distance of 2.88 Å. In contrast, (−)-CBD did not closely approach this residue, maintaining an O–O distance of 3.70 Å, which suggests little to no hydrogen bonding with Ser285. For comparison, the synthetic cannabinoid CP55940 showed an even more favorable docking score (−8.99 kcal/mol) and was found to engage more extensively with lipophilic residues within the receptor pocket. Notably, it formed a strong hydrogen bond with Ser285, with an O–O distance of 2.59 Å.

4 | Discussion

The principal finding of this study is that (+)-CBD is a robust agonist at human CB_2 receptors, in sharp contrast to (−)-CBD, which has little CB_2 activity under these conditions. The effects of (+)-CBD were inhibited by the CB_2 antagonist AM630, blocked by pretreatment of cells with pertussis toxin, and (+)-CBD had no effect on the membrane potential of AtT20-FlpIn cells that were not engineered to express CB_2. (+)-CBD has been reported to have an affinity of 200 nM for CB_2 (species unspecified) in a radioligand binding assay [19, 41], which is similar to the EC_{50} we observed in the assay of cellular membrane potential (235 nM). We are unaware of any other reports of (+)-CBD activity at CB_2 receptors in vitro. One limitation of the assay we used is that (+)-CBD modestly (14%) inhibited GIRK channel activation by ML297 at the highest concentrations tested; this may explain the reduced maximum of CBD compared to the high efficacy agonist CP 55940 (about 10% less). We were also unable to obtain the other 2 isomers of CBD—cis-(3*R*,4*S*)-CBD and cis-(3S,4R)-CBD for testing.

In vivo, (+)-CBD and analogues have been reported to be anticonvulsant and inhibit ovulation in rodent models; however, the receptor(s) involved in these effects were not identified [42, 43]. CBD has been reported to have weak agonist activity in an assay of cAMP accumulation in CHO cells expressing CB_2 ($EC_{50} > 10$ μM) [12], potential allosteric antagonist activity

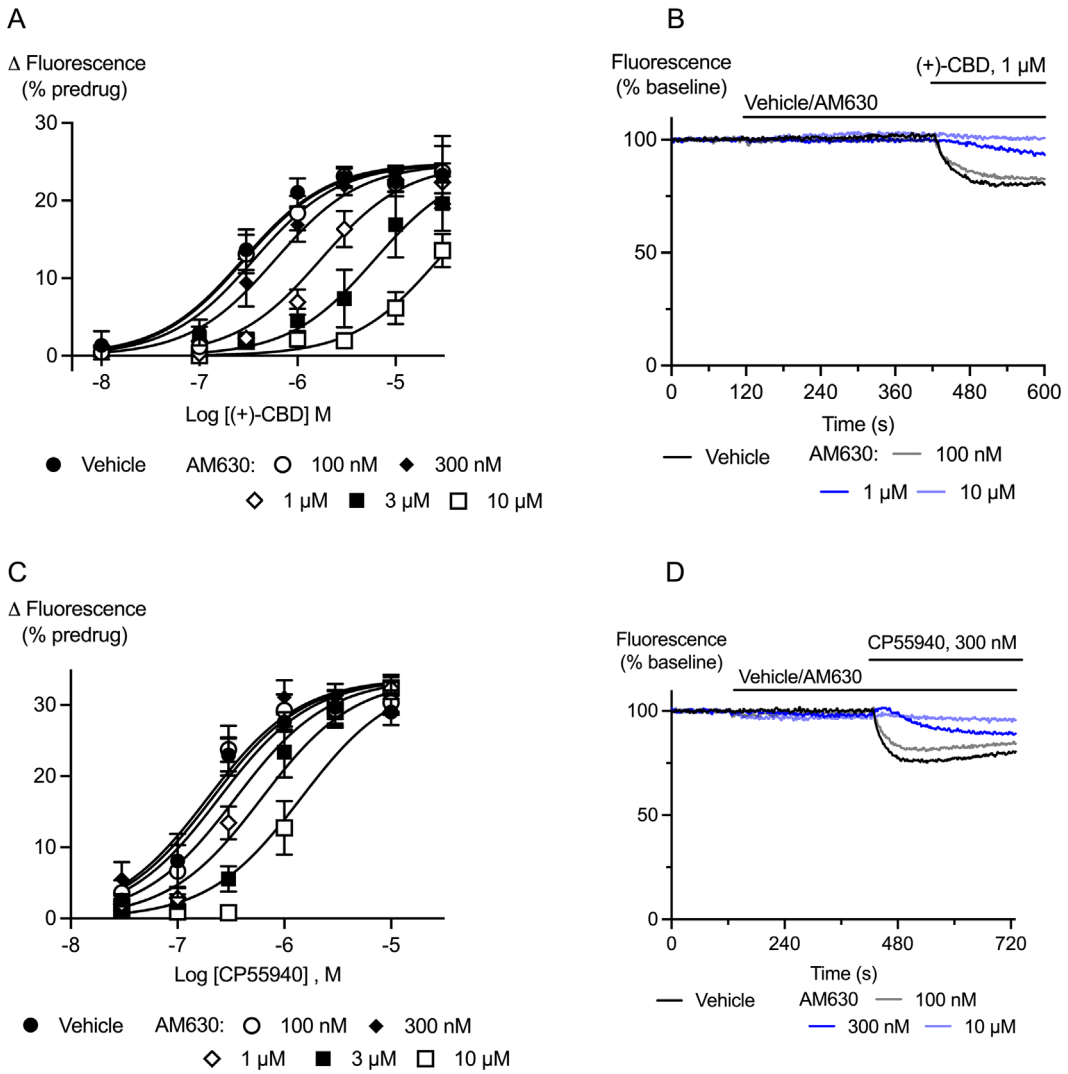

FIGURE 4 | Effects of (+)-CBD and CP55940 are inhibited by the CB_2 antagonist AM630. AtT20 cells expressing CB_2 receptors were preincubated with AM630 (100 nM to 10 μM) and then challenged with (+)-CBD (10 nM—30 μM) or CP55940 (30 nM—10 μM). (A) Represents the pooled concentration response curves for (+)-CBD in the presence of the indicated concentrations of AM630. The curves were shifted in parallel as AM630 concentrations increased (Schild slope 1.1 ± 0.1, pA_2 6.5 ± 0.16, $n = 6$ independent experiments). (B) Example traces showing the progressive reduction in the response to (+)-CBD (1 μM) produced by increasing concentrations of AM630. (C) Represents the pooled concentration response curves for CP55940 in the presence of the indicated concentrations of AM630. The curves were shifted in parallel as AM630 concentrations increased (Schild slope 0.9 ± 0.1, pA_2 6.0 ± 0.17, $n = 6$ independent experiments). (D) Example traces showing the progressive reduction in the response to CP55940 (300 nM) produced by increasing concentrations of AM630.

in an assay of GTPγS binding in CB_2 receptor expressing CHO cells [10] and in cAMP accumulation assays in HEK293 cells expressing CB_2 [13]. All these experiments appear to have been carried out with plant-derived, presumably (−)-CBD. A study by Moniruzzaman and colleagues [44] reported that synthetic CBD inhibited the proliferation and migration of several colon cancer cell lines in a manner that was sensitive to the CB_2 antagonist SR144528, and in one case the CB_1 antagonist AM251. The concentrations of CBD used were quite high (5 μg.mL^{-1} minimum, or about 16 μM), but the results are consistent with what is reported here if the synthetic CBD was a racemic mixture or even pure (+)-CBD.

(+)-CBD had modest activity at CB_1 and after brief preincubation it diminished the effects of CP55940, consistent with a moderate affinity and low efficacy at this receptor. At rat CB_1, (+)-CBD has been reported to have an affinity of 250 nM–840 nM [19, 21, 41] and it acts as a potent antagonist of mouse CB_1 activation in assays of autaptic neurotransmission [21]. We have not tested the effects of (+)-CBD at mouse or rat CB_1 or CB_2 receptors, and it is possible that the effects of (+)-CBD are different at these receptors. It would be worth conducting similar experiments to those reported here at rat and mouse receptors to clarify the relevance of the CB_1 and CB_2 receptor activity of (+)-CBD for studies in preclinical animal models.

Under the same conditions in which (+)-CBD was an effective CB_2 agonist, (−)-CBD had no acute agonist activity and little effect on CP55940 signaling at either CB_1 or CB_2; consistent with its activity as a negative allosteric modulator of CB_1 [10, 11]. The effects of (−)-CBD in cell signaling assays are complex, which may in

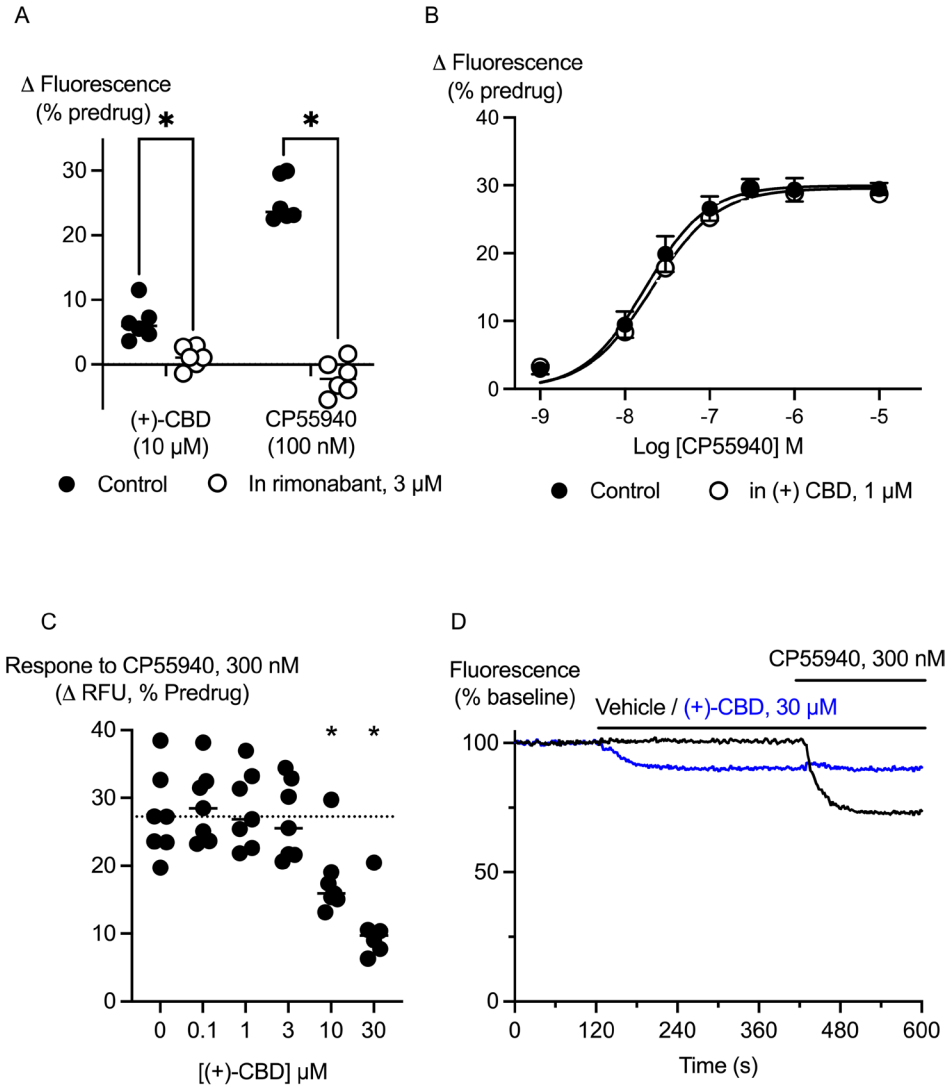

FIGURE 5 | (+)-CBD is a low efficacy, low potency agonist of CB_1 receptors. AtT20 cells expressing CB_1 receptors were preincubated for 5 min with (+)-CBD or rimonabant and challenged with (+)-CBD or CP55940. (A) Preincubation with rimonabant (3 μM) significantly (*) inhibited the effects of (+)-CBD (30 μM) and CP55940 (100 nM; Student's unpaired *t*-test, $p < 0.05$ for each). (B) Preincubation with (+)-CBD, 1 μM, did not affect the concentration response relationship to subsequent application of CP55940 ($n = 6$). (C) preincubation with (+)-CBD (10 μM, 30 μM) significantly (*) inhibited the effects of CP55940 (300 nM; one-way ANOVA, $p < 0.0001$, followed by Dunnett's test for multiple comparisons, $n = 7$). (D) Example traces showing the hyperpolarization of AtT20-CB_1 cells by (+)-CBD, and the subsequent inhibition of the response to CP55940.

part reflect specific interactions with a wide variety of G protein-coupled receptors (and other proteins) as well as unspecific actions caused by effects on cell membranes or even colloidal aggregation by the poorly soluble (−)-CBD [20, 45]. We are confident that the agonist activity of (+)-CBD at CB_2 was specific for a number of reasons. The effect was sensitive to the generally accepted inhibitor of orthosteric CB_2 receptor function, the CB_2 antagonist AM630. Receptor signaling was significantly reduced by pertussis toxin (PTX), an inhibitor of G_i/G_o-type G proteins which are the primary transducers of CB_2 signaling, and (+)-CBD had no effect on membrane potential in AtT20 cells not expressing cannabinoid receptors. Noteworthy, the concentration of (+)-CBD that activated CB_2 receptors was well below those reported to result in aggregation of (−)-CBD [45, 46] and consistent with the reported affinity of (+)-CBD for CB_2 (203 nM, [41]). Further, the n_H for the concentration-dependent activation of CB_2 by (+)-CBD was similar to that of orthosteric agonist CP55940, and not different from 1. This is further evidence for a specific site of action because drugs which are reported to have unspecific effects on receptor activation attributable to their propensity to aggregate in solution often display concentration-response curves with a steep n_H [45].

(+)-CBD appeared to be a low efficacy, low potency agonist at CB_1. The hyperpolarization produced by (+)-CBD was sensitive to the CB_1 antagonist rimonabant and pertussis toxin. High concentrations of (+)-CBD reduced the activation of CB_1 by CP55940, consistent with it being a low efficacy agonist. High concentrations of (+)-CBD (but not (−)-CBD) also inhibited somatostatin-induced hyperpolarization of AtT20 cells, suggesting weak antagonist activity at the endogenous SSTR in AtT20 cells.

Molecular docking simulations suggest that the difference in CB_2 receptor activity between (−)-CBD and (+)-CBD is

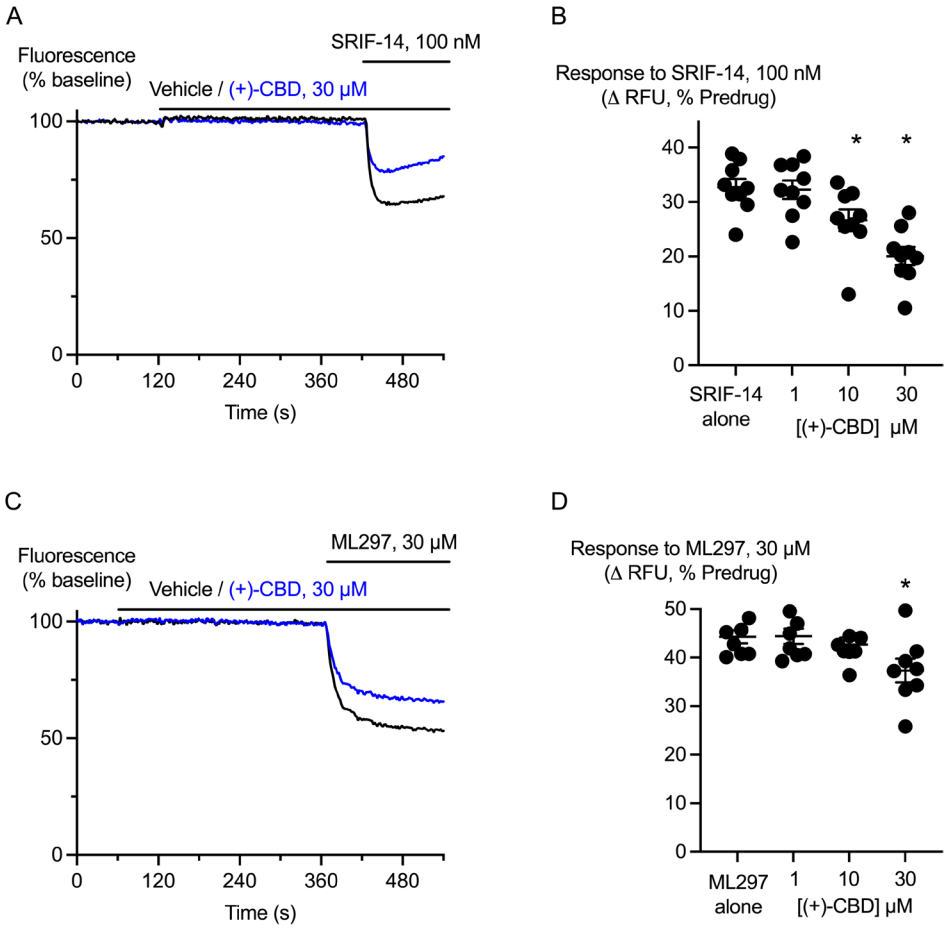

FIGURE 6 | (+)-CBD is a low potency inhibitor of somatostatin receptors and GIRK channels. AtT20-WT cells (expressing neither CB_1 nor CB_2 receptors) were preincubated with (+)-CBD for 5 min and challenged with SRIF-14 (100 nM) or the GIRK activator ML297 (30 μM). (A) Example traces showing that (+)-CBD (30 μM) did not change the membrane potential of AtT20-EV cells, but inhibited their hyperpolarization by SRIF-14. (B) A summary plot of the effects of (+)-CBD on the responses to SRIF-14 (100 nM), (+)-CBD (10 μM, 30 μM) significantly (*) inhibited the responses (one-way ANOVA, $p < 0.0001$, followed by Dunnett's test for multiple comparisons, $n = 8$). (C) Example traces showing that (+)-CBD (30 μM) inhibited the hyperpolarization of AtT20-WT cells by ML297. (D) A summary plot of the effects of (+)-CBD on the responses to ML297 (30 μM), (+)-CBD (30 μM) significantly (*) inhibited the responses (one-way ANOVA, $p = 0.0253$, followed by Dunnett's test for multiple comparisons, $n = 8$).

primarily driven by differences in binding affinity and enhanced interaction with a residue important for CB_2 activation. (+)-CBD, which exhibited a more negative docking score, is predicted to form more energetically favorable interactions with CB_2, and thus demonstrates higher affinity. Similarly, CP55940 showed an even more favorable docking score than both CBD enantiomers, consistent with its experimentally observed high binding affinity for CB_2 [30]. A key factor contributing to the differential affinity appears to be the ability of the compounds to form hydrogen bonds with the serine residue at position 285 (Ser285). Previous mutagenesis studies have shown that Ser285 plays a critical role in ligand binding and agonist activity for some cannabinoid-like compounds, including CP55940 [30]. Both CP55940 and (+)-CBD form hydrogen bonds with Ser285, with CP55940 exhibiting a particularly strong interaction, indicated by a short O–O distance of 2.59 Å (Figure 6C). (+)-CBD also forms a moderately strong hydrogen bond with Ser285 (O–O distance of 2.88 Å) (Figure 6B). In contrast, (−)-CBD, due to its enantiomeric configuration, fails to position its phenolic oxygen close enough to Ser285 to form a meaningful interaction (Figure 6A). With an O–O distance of 3.70 Å, simulations suggest only a weak or negligible hydrogen bond between (−)-CBD and Ser285. These findings indicate that the enantiomeric configuration in the CBD structure can significantly influence how different functional groups orient within the CB_2 receptor binding pocket and directly impact receptor affinity.

To our knowledge only one study has reported the effects of administration of (+)-CBD to humans [23]. That study used robust doses of (+)-CBD (200 mg–800 mg) administered before a cold pressor test to measure effects on pain thresholds and pain tolerance when compared with placebo. There were small or insignificant effects of (+)-CBD on acute pain threshold or tolerance, although all doses increased the perceived painfulness of the stimulus. (+)-CBD did not affect the subjective mood or the heart rate of participants, which are canonical effects of CB1 agonist administration in humans [47]. This is consistent with the limited activity of (+)-CBD at CB_1 we measured, but (+)-CBD did produce a small but significant decrease in blood pressure in humans [23]. Overall, (+)-CBD was well tolerated, similar to other CB_2 agonists trialed in

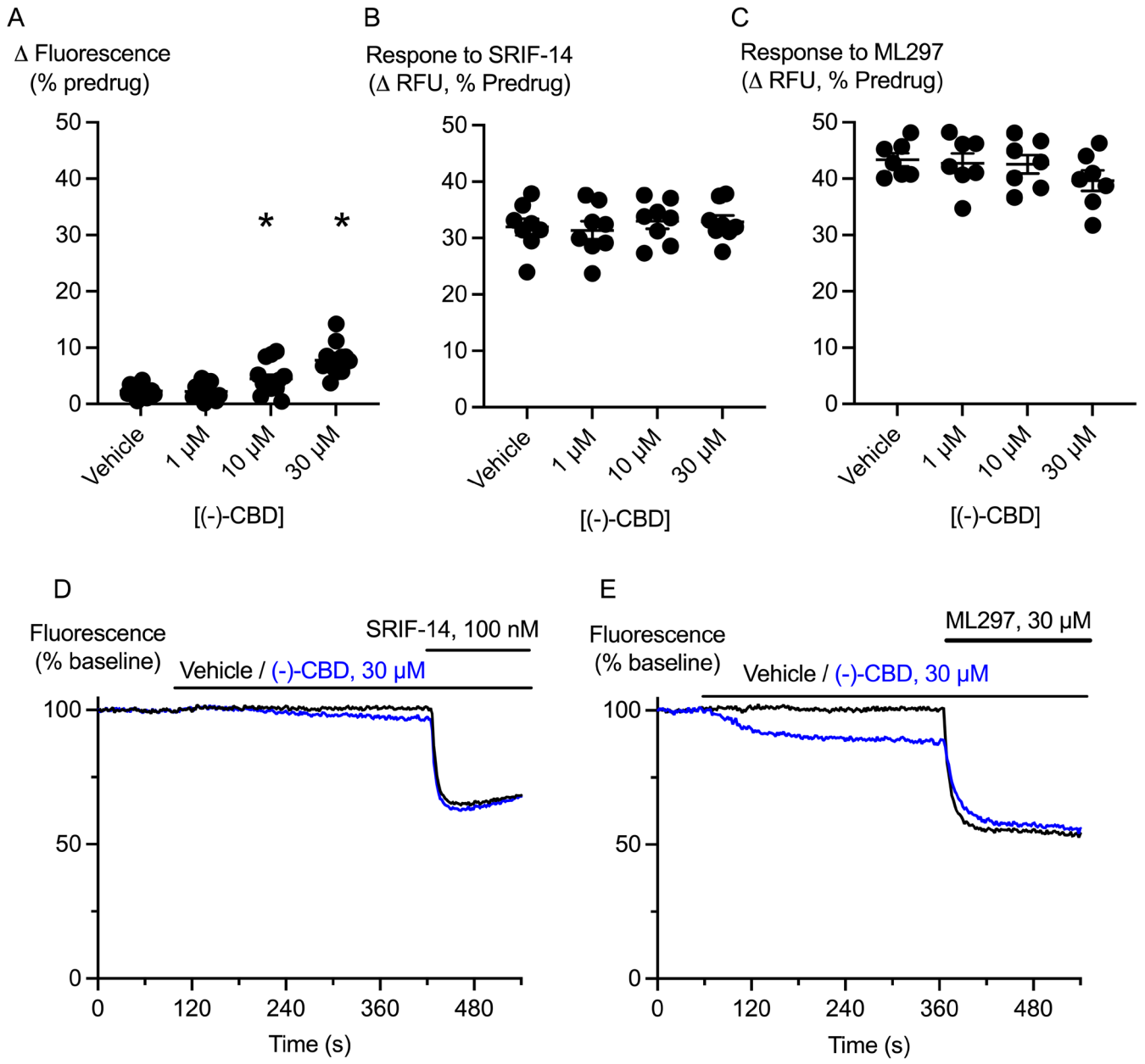

FIGURE 7 | (–)-CBD has distinct effects to (+)-CBD in cells not expressing cannabinoid receptors. AtT20-WT cells were incubated with (–)-CBD for 5 min and then challenged with SRIF-14 (100 nM) or the GIRK activator ML297 (30 μM). (A) A summary plot of the effects of (–)-CBD alone on the fluorescence of AtT20-WT cells, (–)-CBD (10 μM, 30 μM) produced a significant (*) apparent hyperpolarization of the cells compared to vehicle (one-way ANOVA, $p = 0.0001$, followed by Dunnett's test for multiple comparisons, $n = 15$). (B) (–)-CBD did not inhibit the response of AtT20-WT cells to SRIF-14 (100 nM) (one-way ANOVA, $p = 0.8344$, $n = 8$). (C) (–)-CBD did not inhibit the response of AtT20-WT cells to ML297 (30 μM) (one-way ANOVA, $p = 0.3869$, $n = 7$). (D) Example traces showing the effect (–)-CBD (30 μM) on SRIF-14 responses. (E) Example traces showing the effect (–)-CBD (30 μM) on ML297 responses.

humans. The limited effect of acute administration of a CB_2 agonist on pain responses is perhaps not surprising, given the limited expression of CB2 receptors in human sensory neurons, and the lack of evidence of expression on central neurons involved in pain responses (in humans). It should be noted that many clinical trials using CBD do not specify the molecular identity of the drug, and it is possible that trials using synthetic CBD are administering either racemic mixtures of CBD or indeed simply (+)-CBD.

This study emphasizes the importance of understanding the molecular actions of the enantiomers of chiral cannabinoids. Unlike THC and CBC, there does not seem to be any evidence for the occurrence of (+)-CBD in *Cannabis* plants, but synthetic CBD may have reasonably robust CB_2 agonist activity if it contains a substantial amount of (+)-CBD. Although the safety of (+)-CBD cannot simply be assumed to be the same as (–)-CBD, the identification of (+)-CBD as a robust CB2 agonist suggests that (+)-CBD may be worth exploring as a

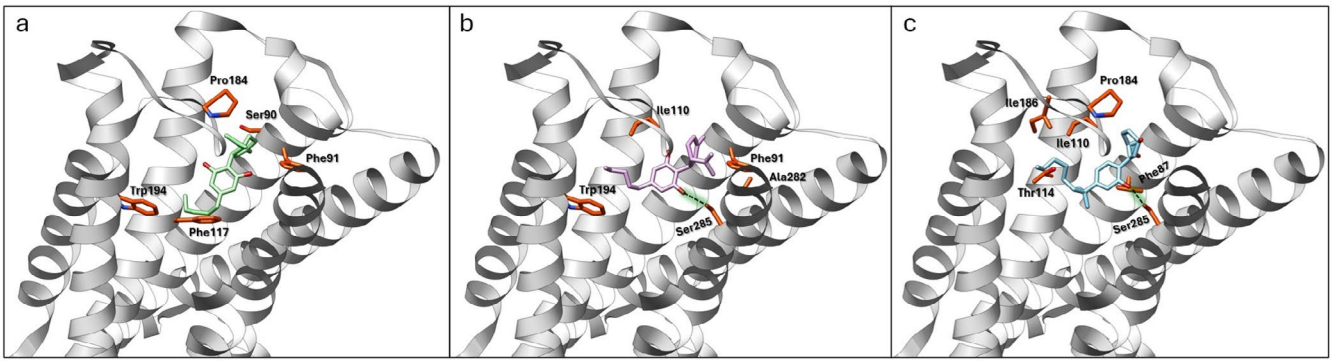

FIGURE 8 | Top energetically favorable 3D binding poses of (−)-CBD (a), (+)-CBD (b), and CP55940 (c) inside the CB2 receptor pocket. Some key surrounding amino acids stabilizing the interaction of the CB2 receptor with the ligand are highlighted in orange. H-bonds between Ser285 and ligands are shown by dashed black lines in b and c. Some residues are omitted for clarity.

therapeutic agent in chronic inflammatory conditions or other diseases where CB_2 activation may prove beneficial.

Author Contributions

Pedro Bans Burtchaell: investigation, formal analysis, writing – original draft, writing – review and editing. **Marina Junqueira Santiago:** investigation, writing – review and editing, formal analysis, supervision, conceptualization, methodology, writing – original draft. **Chenxi Wang:** investigation, formal analysis, writing – review and editing. **Mehdi Hagdoost:** investigation, writing – original draft, writing – review and editing, visualization. **Evie J. M. Clay:** investigation, formal analysis, writing – review and editing. **Dani Mohnot:** investigation, formal analysis, writing – review and editing. **Mark Connor:** conceptualization, investigation, writing – original draft, writing – review and editing, formal analysis, supervision, visualization, funding acquisition.

Acknowledgments

We thank A/Prof Alf Garcia-Barnett and Prof Alison Rodger for help with the CD determinations. This work was supported by recurrent research funding to M.C. and by the Australian Research Council Industrial Transformation Center for Facilitated Advancement of Australia's Bioactives (Grant IC210100040) and Research Attraction and Acceleration Program funding from the Office of the Chief Scientist and Engineer, Investment NSW. Open access publishing facilitated by Macquarie University, as part of the Wiley - Macquarie University agreement via the Council of Australasian University Librarians.

Funding

This work was supported by the Australian Research Council, IC210100040. Office of the Chief Scientist and Engineer, Investment NSW.

Conflicts of Interest

Medhi Hagdoost is an employee of Nalu Bio. This work was done in his private capacity, and there is no relationship between Nalu Bio and the other authors. The authors declare no other potential conflicts of interest.

Data Availability Statement

The data that support the findings of this study are available from the corresponding author upon reasonable request.

References

1. A. Bilbao and R. Spanagel, "Medical Cannabinoids: A Pharmacology-Based Systematic Review and Meta-Analysis for All Relevant Medical Indications," *BMC Medicine* 20, no. 1 (2022): 259, https://doi.org/10.1186/s12916-022-02459-1.

2. H. R. Ross, I. Napier, and M. Connor, "Inhibition of Recombinant Human T-Type Calcium Channels by Δ^9-Tetrahydrocannabinol and Cannabidiol," *Journal of Biological Chemistry* 283 (2008): 16124–16134.

3. M.-R. Ghovanloo, N. G. Shuart, J. Mezeyova, R. A. Dean, P. C. Ruben, and S. J. Goodchild, "Inhibitory Effects of Cannabidiol on Voltage-Dependent Sodium Currents," *Journal of Biological Chemistry* 293, no. 43 (2018): 16546–16558, https://doi.org/10.1074/jbc.RA118.004929.

4. H. X. B. Zhang, L. Heckman, Z. Niday, et al., "Cannabidiol Activates Neuronal Kv7 Channels," *eLife* 18, no. 11 (2022): e73246, https://doi.org/10.7554/eLife.73246.

5. E. Billard, A. Torbey, A. Inserra, et al., "Pharmacological Characterization of Cannabidiol as a Negative Allosteric Modulator of the 5-HT2A Receptor," *Cellular Signalling* 127 (2025): 111588, https://doi.org/10.1016/j.cellsig.2025.111588.

6. J. S. Kaplan, N. Stella, W. A. Catterall, and R. E. Westenbroek, "Cannabidiol Attenuates Seizures and Social Deficits in a Mouse Model of Dravet Syndrome," *Proc Natl Acad Sci USA* 114, no. 42 (2017): 11229–11234, https://doi.org/10.1073/pnas.1711351114.

7. E. B. Russo, A. Burnett, B. Hall, and K. K. Parker, "Agonistic Properties of Cannabidiol at 5-HT1a Receptors," *Neurochemical Research* 30 (2005): 1037–1043.

8. P. N. Patsalos, J. Szaflarski, B. Gidal, K. Van Landingham, D. Critchley, and G. Morrison, "Clinical Implications of Trials Investigating Drug-Drug Interactions Between Cannabidiol and Enzyme Inducers or Inhibitors or Common Antiseizure Drugs," *Epilepsia* 61, no. 9 (2020): 1854–1868, https://doi.org/10.1111/epi.16674.

9. S. M. Stout and N. M. Cimino, "Exogenous Cannabinoids as Substrates, Inhibitors, and Inducers of Human Drug Metabolizing Enzymes: A Systematic Review," (2013), https://doi.org/10.3109/03602532.2013.849268.

10. A. Thomas, G. L. Baillie, A. M. Phillips, R. K. Razdan, R. A. Ross, and R. G. Pertwee, "Cannabidiol Displays Unexpectedly High Potency as an Antagonist of CB_1 and CB_2 Receptor Agonists *in Vitro*," *British Journal of Pharmacology* 150, no. 5 (2007): 613–623, https://doi.org/10.1038/sj.bjp.0707133.

11. R. B. Laprairie, A. M. Bagher, M. E. M. Kelly, and E. M. Denovan-Wright, "Cannabidiol Is a Negative Allosteric Modulator of the

Cannabinoid CB1 Receptor," *British Journal of Pharmacology* 172 (2015): 4790–4805, https://doi.org/10.1111/bph.13250.

12. A. Zagzoog, K. A. Mohamed, H. J. J. Kim, et al., "In Vitro and In Vivo Pharmacological Activity of Minor Cannabinoids Isolated From *Cannabis sativa*," *Scientific Reports* 10 (2020): 20405, https://doi.org/10.1038/s41598-020-77175-y.

13. E. Martinez-Pinilla, K. Varani, I. Reyes-Resina, et al., "Binding and Signaling Studies Disclose a Potential Allosteric Site for Cannabindiol in Cannabinoid CB2 Receptors," *Frontiers in Pharmacology* 8 (2017): 744, https://doi.org/10.3389/fphar.2017.00744.

14. J. Bouma, J. D. Broekhuis, C. Cas van der Horst, et al., "Dual Allosteric and Orthosteric Pharmacology of Synthetic Analog Cannabidiol-Dimethylheptyl, but Not Cannabidiol, on the Cannabinoid CB2 Receptor," *Biochemical Pharmacology* 218 (2023): 115924, https://doi.org/10.1016/j.bcp.2023.115924.

15. V. K. Rao, M. M. Lewis-Bakker, E. Wasilewski, H. A. Clarke, and L. P. Kotra, "Stereoisomers of Cannabidiols and Their Pharmacological Activities – A Potentially Novel Direction for Cannabinoids," *Bioorganic & Medicinal Chemistry* 117 (2025): 118019, https://doi.org/10.1016/j.bmc.2024.118019.

16. G. Mazzoccanti, O. H. Ismail, I. D'Acquarica, et al., "Cannabis Through the Looking Glass: Chemo- and Enantio-Selective Separation of Phytocannabinoids by Enantioselective Ultra High Performance Supercritical Fluid Chromatography," *Chemical Communications* 53 (2017): 12262–12265, https://doi.org/10.1039/C7CC06999E.

17. M. A. Schafroth, G. Mazzoccanti, I. Reynoso-Moreno, et al., "Δ^9-Cis-Tetrahydrocannabinol: Natural Occurrence, Chirality, and Pharmacology," *Journal of Natural Products* 84, no. 9 (2021): 2502–2510, https://doi.org/10.1021/acs.jnatprod.1c00513.

18. A. Calcaterra, G. Cianfoni, C. Tortora, et al., "Natural Cannabichromene (CBC) Shows Distinct Scalemicity Grades and Enantiomeric Dominance in *Cannabis sativa* Strains," *Journal of Natural Products* 86, no. 4 (2023): 909–914, https://doi.org/10.1021/acs.jnatprod.2c01139.

19. L. O. Hanus, S. Tchilibon, D. E. Ponde, A. Breuer, E. Fride, and R. Mechoulam, "Enantiomeric Cannabidiol Derivatives: Synthesis and Binding to Cannabinoid Receptors," *Organic & Biomolecular Chemistry* 3, no. 6 (2005): 1116–1123, https://doi.org/10.1039/b416943c.

20. K. M. Nelson, J. Bisson, G. Singh, et al., "The Essential Medicinal Chemistry of Cannabidiol (CBD)," *Journal of Medicinal Chemistry* 63 (2020): 12137–12155, https://doi.org/10.1021/acs.jmedchem.0c00724.

21. T. Bosquez-Berger, S. Wilson, C. Iliopoulos-Tsoutsouvas, et al., "Differential Enantiomer-Specific Signaling of Cannabidiol at CB1 Receptors," *Molecular Pharmacology* 102, no. 6 (2022): 259–268, https://doi.org/10.1124/molpharm.121.000305.

22. J. C. Arnold, D. McCartney, A. Suraev, and I. S. McGregor, "The Safety and Efficacy of Low Oral Doses of Cannabidiol: An Evaluation of the Evidence," *Clinical and Translational Science* 16, no. 1 (2023): 10–30, https://doi.org/10.1111/cts.13425.

23. C. A. Arout, M. Haney, E. S. Herrmann, G. Bedi, and Z. D. Cooper, "A Placebo-Controlled Investigation of the Analgesic Effects, Abuse Liability, Safety and Tolerability of a Range of Oral Cannabidiol Doses in Healthy Humans," *British Journal of Clinical Pharmacology* 88, no. 1 (2022): 347–355, https://doi.org/10.1111/bcp.14973.

24. H. Edery, Y. Grunfeld, Z. Ben-Zvi, and R. Mechoulam, "Structural Requirements for Cannabinoid Activity," *Annals. New York Academy of Sciences* 191 (1971): 40–53, https://doi.org/10.1111/j.1749-6632.1971.tb13985.x.

25. M. Udoh, M. Santiago, S. Haneef, et al., "Activation of CB_2 Receptors by (−)-Cannabichromene but Not (+)-Cannabichromene," *Cannabis and Cannabinoid Research* 10, no. 1 (2025): e94–e101, https://doi.org/10.1089/can.2023.0212.

26. S. P. H. Alexander, A. P. Davenport, E. Kelly, et al., "The Concise Guide to PHARMACOLOGY 2025/26: G Protein-Coupled Receptors," *British Journal of Pharmacology* 182 (2025): S24–S151.

27. S. D. Banister, M. Longworth, R. Kevin, et al., "Pharmacology of Valinate and Tert-Leucinate Synthetic Cannabinoids 5F-AMBICA, 5F-AMB, 5FADB, AMB-FUBINACA, MDMB-FUBINACA, MDMB-CHMICA, and Their Analogues," *ACS Chemical Neuroscience* 7, no. 9 (2016): 1241–1254, https://doi.org/10.1021/acschemneuro.6b00137.

28. A. Knapman, M. Santiago, Y.-P. Du, P. Bennallack, M. J. Christie, and M. Connor, "A Continuous, Fluorescence-Based Assay of μ-Opioid Receptor Activation in AtT-20 Cells," *Journal of Biomolecular Screening* 18, no. 3 (2013): 269–276, https://doi.org/10.1177/1087057111246137.

29. C. Xing, Y. Zhuang, T.-H. Xu, et al., "Cryo-EM Structure of the Human Cannabinoid Receptor CB2-G_i Signaling Complex," *Cell* 180, no. 4 (2020): 645–654, https://doi.org/10.1016/j.cell.2020.01.007.

30. X. Li, C. Chang, J. Bouma, et al., "Structural Basis of Selective Cannabinoid CB_2 Receptor Activation," *Nature Communications* 14, no. 1 (2023): 1447, https://doi.org/10.1038/s41467-023-37112-9.

31. T. Hua, X. Li, L. Wu, et al., "Activation and Signaling Mechanism Revealed by Cannabinoid Receptor-G_i Complex Structures," *Cell* 180, no. 4 (2020): 655–665, https://doi.org/10.1016/j.cell.2020.01.008.

32. B. J. Bender, S. Gahbauer, A. Luttens, et al., "A Practical Guide to Large-Scale Docking," *Nature Protocols* 16 (2021): 4799–4832, https://doi.org/10.1038/s41596-021-00597-z.

33. M. V. Shapalov and R. L. Dunbrack, "A Smooth Back-Bone-Dependent Rotamer Library for Proteins Derived From Adaptive Kernel Density Estimates and Regressions," *Structure* 19, no. 6 (2011): 844–858, https://doi.org/10.1016/j.str.2011.03.019.

34. P. Banas, D. Hollas, M. Zgarbova, et al., "Performance of Molecular Mechanics Force Fields for RNA Simulations: Stability of UUCG and GNRA Hairpins," *Journal of Chemical Theory and Computation* 6, no. 12 (2010): 3836–3849, https://doi.org/10.1021/ct100481h.

35. G. M. Morris, R. Huey, W. Lindstrom, et al., "Autodock4 and AutodockTools4: Automated Docking With Selective Receptor Flexibility," *Journal of Computational Chemistry* 30, no. 16 (2009): 2785–2791, https://doi.org/10.1002/jcc.21256.

36. S. Kim, J. Chen, T. Cheng, et al., "PubChem 2025 Update," *Nucleic Acids Research* 53, no. D1 (2024): D1516–D1525, https://doi.org/10.1093/nar/gkae1059.

37. T. A. Halgren, "Merck Molecular Force Field. I. Basis, Form, Scope, Parameterization, and Performance of MMFF94," *Journal of Computational Chemistry* 17, no. 5–6 (1996): 490–519, https://doi.org/10.1002/(SICI)1096-987X(199604)17:5/6<490::AID-JCC1>3.0.CO;2-P.

38. J. Eberhardt, D. Santos-Martins, A. F. Tillack, and S. Forli, "AutoDock Vina 1.2.0: New Docking Methods, Expanded Force Field and Python Bindings," *Journal of Chemical Information and Modeling* 61, no. 8 (2021): 3891–3898, https://doi.org/10.1021/acs.jcim.1c00203.

39. R. Quiroga and M. A. Villarreal, "Vinardo: A Scoring Function Based on Autodock Vina Improves Scoring, Docking and Virtual Screening," *PLoS One* 11, no. 5 (2016): e0155183, https://doi.org/10.1371/journal.pone.0155183.

40. T. N. H. Pham, T. H. Nguyen, N. M. Tam, et al., "Improving Ligand-Ranking of AutoDock Vina by Changing the Empirical Parameters," *Journal of Computational Chemistry* 43, no. 3 (2022): 160–169, https://doi.org/10.1002/jcc.26779.

41. T. Bisogno, L. Hanus, L. De Petrocellis, et al., "Molecular Targets for Cannabidiol and Its Synthetic Analogues: Effect on Vanilloid VR1 Receptors and on the Cellular Uptake and Enzymatic Hydrolysis of

Anandamide," *British Journal of Pharmacology* 134, no. 4 (2001): 845–852, https://doi.org/10.1038/sj.bjp.0704327.

42. T. Cordova, D. Ayalon, N. Lander, et al., "The Ovulation Blocking Effect of Cannabinoids: Structure-Activity Relationships," *Psychoneuroendocrinology* 5, no. 1 (1980): 53–63, https://doi.org/10.1016/0306-4530(80)90009-8.

43. J. R. Liete, E. A. Carlini, N. Lander, and R. Mechoulam, "Anticonvulsant Effects of the (–) and (+)isomers of Cannabidiol and Their Dimethylheptyl Homologs," *Pharmacology* 24, no. 3 (1982): 141–146, https://doi.org/10.1159/000137588.

44. M. Moniruzzaman, K. Y. Wong, T. I. Janjua, J. H. Martin, J. Begun, and A. Popat, "Cannabidiol Targets Colorectal Cancer Cells via Cannabinoid Receptor 2, Independent of Common Mutations," *ACS Pharmacology & Translational Science* 8, no. 2 (2025): 543–556, https://doi.org/10.1021/acsptsci.4c00644.

45. P. S. Cogan, "A Cautionary Tale of Paradox and False Positives in Cannabidiol Research," *Expert Opinion on Drug Discovery* 20, no. 1 (2025): 5–15.

46. A. D'Aloia, M. Ceriani, R. Tisi, S. Stucchi, E. Sacco, and B. Costa, "Cannabidiol Antiproliferative Effect in Triple-Negative Breast Cancer MDA-MB-231 Cells Is Modulated by Its Physical State and by IGF-1," *International Journal of Molecular Sciences* 23, no. 13 (2022): 7145, https://doi.org/10.3390/ijms23137145.

47. M. A. Huestis, D. A. Gorelick, S. J. Heishman, et al., "Blockade of the Effects of Smoked Marijuana by the CB1-Selective Antagonist SR141716," *Archives of General Psychiatry* 58, no. 4 (2001): 322–328, https://doi.org/10.1001/archpsyc.58.4.322.

Supporting Information

Additional supporting information can be found online in the Supporting Information section. **Figure S1:** (–)-CBD and (+)-CBD used in this study have distinct optical spectra. The absorbance and circular dichroism (CD) spectra of the samples were determined on a Jasco (Hachioji, Japan) J-1500 spectropolarimeter by diluting the enantiomerically pure sample to 0.1 mg.mL^{-1} in ethanol, with 0.1 mm path length. (A and C) CD spectra and (B and D) absorbance spectra of (–)-CBD and (+)-CBD.